Diyala Journal of Engineering Sciences

Journal homepage: https://djes.info/index.php/djes

ISSN: 1999-8716 (Print); 2616-6909 (Online)

# Enhancing Wind Turbine Stability and Performance: A Case Study on Speed Control and Maximum Power Point Tracking

Muhammad Qasim Nawaz, Wei Jiang* and Aimal Khan

Department of Electrical Engineering and Automation, Yangzhou University, 225127 Yangzhou, China

**ARTICLE INFO**

***Article history:***
Received October 22, 2023
Revised February 19, 2024
Accepted February 22, 2024
Available online March 5, 2024

***Keywords:***
Wind turbine stability
Wind turbine performance
Speed control
Maximum power point tracking
Near-zero implementation

**ABSTRACT**

Wind turbine performance is a critical aspect of renewable energy systems, and this study focuses on optimizing it through innovative strategies. It also discussed the different parts of WECS, such as wind turbines, generators, and control systems, to enhance their performance and efficiency. The research delves into the integration of speed control and Maximum Power Point Tracking (MPPT) mechanisms using a sophisticated Three-Phase Interleaved Buck-Boost Converter. The converter's unique topology, involving a back-to-back connection, shows a pivotal part in shaping the performance of the wind turbine. Furthermore, the near-zero implementation in MPPT strives to minimize oscillations and enhance photovoltaic panel and wind turbine efficiency. This technique, as explored in various studies, aims to achieve stable, efficient power output by reducing perturbations, ensuring optimal energy capture, and improving overall system reliability. This study investigates the transformation before and after near-zero implementation in various contexts. It explores the impact on energy efficiency with near-zero properties, and the performance of buildings, providing insights into the substantial changes brought about by near-zero initiatives. Additionally, the implementation of MPPT is explored, demonstrating that adjusting delta values can lead to faster stabilization times. By changing the negative delta value to -0.0005, the system achieves stabilization at the target power of 19 kW within 0.2 seconds. These findings emphasize the versatility of the Three-Phase Interleaved Buck-Boost Converter in enhancing both speed control and MPPT for wind turbines.

## 1. Introduction

Renewable energy sources for example wind energy are growing in the space due to rising prices, increasing demand for natural gas and limited supplies. Moreover renewable energy sources are becoming increasingly important as we strive to reduce carbon emissions and become more environmentally sustainable. Wind energy is one such source that has shown great potential in recent years [1]. In 2022, the world's new wind energy installation capacity will be approximately 77.6 GW. Onshore wind still accounts for the largest share of wind energy, but offshore wind has increased rapidly in recent years as shown in Figure 1. In 2022, the world's cumulative wind energy installation capacity will be approximately 906 GW. Onshore wind energy accounted for the majority of all wind energy installations that year, approximately 842 GW as shown in Figure 2. The world's largest wind energy market is China, with over 237 GW of wind energy installation capacity. China has a very large surface area, long coastline and great climate potential [2]. This includes 9% year-on-year growth. 2023 will be the year when new global capacity will exceed 100 GW for the first time, with GWEC Business Intelligence forecasting 15% annual growth [3].

*Corresponding author.
E-mail address: jiangwei@yzu.edu.cn
DOI: 10.24237/djes.2024.17101

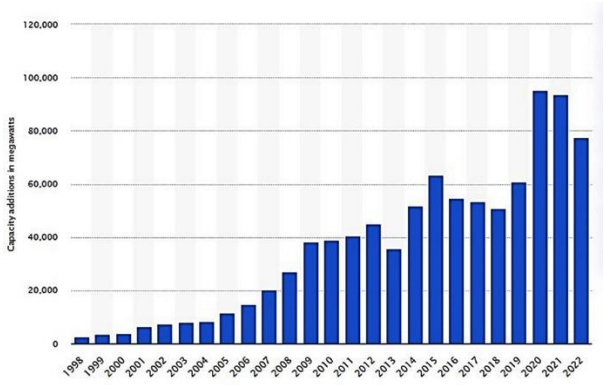


**Figure 1.** Annual wind power capacity installed worldwide from 1998 to 2022 [1]

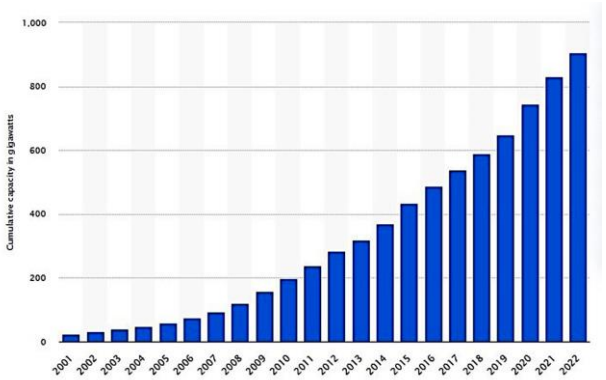


**Figure 2.** Global cumulative wind energy installed capacity from 2001 to 2022 [2]

Recent research has delved into comparative analyses of MPPT techniques, offering valuable insights into improving efficiency in wind production systems [4]. In this paper the focus of this scheme is to develop and implement a system for controlling the speed of a wind turbine to optimize its output power. To determine a turbine's characteristics, the strategy starts with a plot of the turbine's power output at various shaft speeds. This solution uses a stable synchronous generator to convert mechanical energy into electrical energy and study the power output $P_{output}$ of the wind turbine at different poles. The product of rotational speed $\omega_{rotational}$ and torque $T$ determines a wind turbine's output power [5].

$$P_{output} = T \times \omega_{rotational} \quad (1)$$

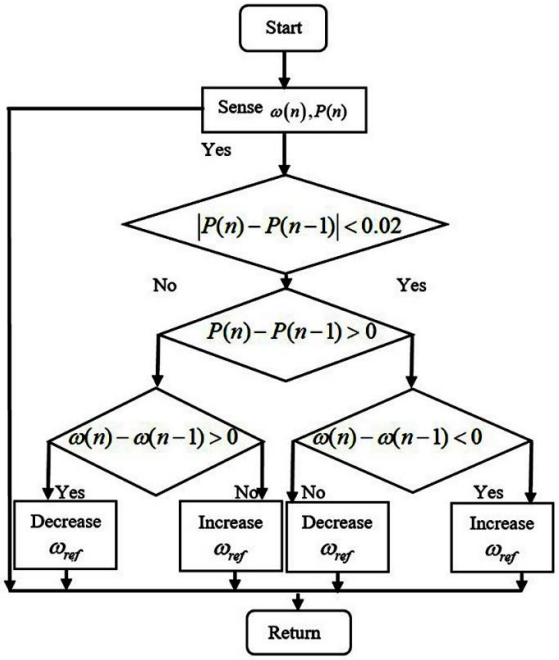


**Figure 3.** Flow chart of the perturbation and observation algorithm for wind turbine [7]

Torque is a measure of the winding force that causes the shaft to rotate, and directly proportional to wind power on the blades. Rotational speed, on the other hand, is the speed at which the shaft is rotating, and it is directly proportional to the wind speed. A diode bridge rectifies the AC signal to DC, which is then smoothed using a capacitor [6]. The next step is to use a three-phase interleaved buck-boost converter for speed control, which can regulate power output to match desired output power quickly. The reason for the use of interleaved Buck-Boost converters is that it has enhanced efficiency, power density, and dynamic response while minimizing ripples and improving heat transfer [7]. Furthermore, two controllers with optimized gain values are used in a Proportional-Integral (PI) loop to adjust the duty cycle of the converter, combining proportional and integral controls to minimize overshoot and provide a stable system. The input speed, measured by the shaft speed, is adjusted to match multiple input speeds, and the system is tested for performance [8]. The flow of power through in WECS the circuit is represented in Figure 4. Using perturbations and observations, the next challenge is to implement maximum power point tracking (MPPT).

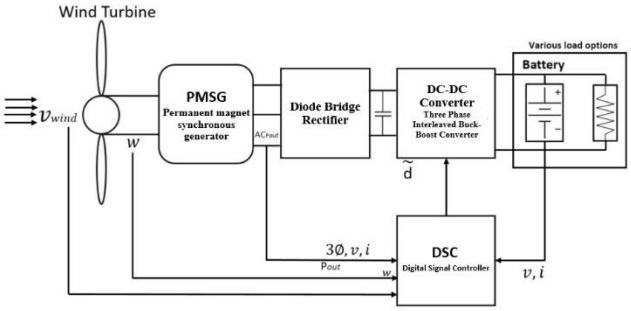


**Figure 4.** Block Diagram Showing Flow of Power through WECS System [8]

The goal of MPPT is to regulate wind turbine speed in order to sustain maximum power output. Different perturbation delta values are tested to fine-tune the system, and the wind turbine's speed is changed from $12m/s$ to $8m/s$ [9-10]. Figure 5 shows the schematic wind turbine system with a phase interleaved Buck-Boost converter and the MPPT algorithm control block diagram is shown in Figure 6. This scheme is relevant because optimizing wind energy production is essential in our transition to renewable energy sources. By controlling the wind turbine's speed, its power output can be maximized, thereby increasing its efficiency and reducing our reliance on non-renewable energy sources [11-12].

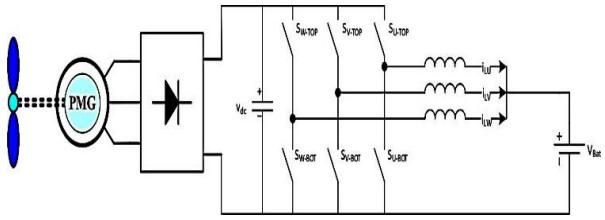


**Figure 5.** Wind Turbine System with three Phase Interleaved Buck-Boost Converter [11]

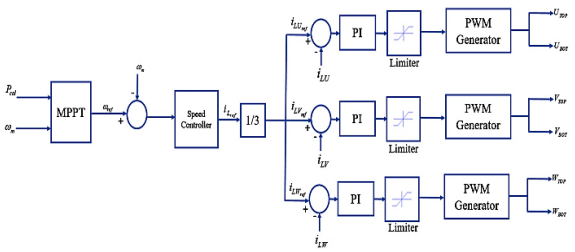


**Figure 6.** Control Block Diagram for MPPT Algorithm [12]

## 2. Literature review

This literature review on improving wind turbine stability and efficiency through speed control and maximum power point finding (MPPT) is a research project to optimize wind energy collectors. Researchers have focused on the role of the MPPT controller in driving wind energy harvesting systems at the maximum speed, equivalent to the optimum power at various wind speeds [12]. Effective speed control mechanisms are essential for adapting the turbine to varying wind speeds. Literature suggests that employing interleaved buck-boost converters enables precise regulation, mitigating the impact of wind fluctuations [13,14]. MPPT is vital for maximizing energy extraction. Studies highlight the significance of interleaved buck-boost converters in MPPT strategies, ensuring efficient power transfer from the wind to the electrical system [15,16]. The integration of speed control and MPPT with interleaved buck-boost converters offers a synergistic approach. This combination enhances the turbine's stability, efficiency, and overall performance, contributing to the advancement of wind energy systems [17]-[18]. In the context of wind turbine control, generator torque control plays a pivotal role in varying the rotor speed based on MPPT approaches for extracting maximum power from the wind [19]. The literature explores various MPPT algorithms and control strategies, including optimal torque control, tipspeed ratio control, and power signal-based control, discussing their efficacy in wind energy conversion systems [20]. In addition, the paper explores particular MPPT algorithms that dynamically modify generator control and rotor speed in order to continuously follow the wind and harvest its maximum power, offering insights into the intricate balance required for efficient energy extraction [21]. This paper shows advances such as changes in interference and analysis algorithms based on the trapezoidal law, which demonstrate new ways of tracking wind peaks in electronic systems [22]. Collectively, this literature review also provides a comprehensive understanding of the various MPPT techniques and control strategies employed to enhance

wind turbine stability and performance, contributing to the ongoing efforts in sustainable wind energy utilization [23].

## 3. Generators in wind energy conversion system

WECS uses multiple generators. Squirrel cage asynchronous generators (SCIGs) can be considered as a low-cost, reliable, and convenient option for WECS [24]. As a component of Wind Energy Conversion Systems, a constant speed wind turbine with a squirrel cage induction generator (SCIG) runs at a constant rotor speed (WECS). Studies have explored reduced-order models for these generators, improving understanding and control of these systems as shown in Figure 7(a). Doubly-fed asynchronous generators (DFIG) are also preferred for WECS because they are very efficient when used with transformers. Their only problem is that they need a multistage gearbox, and they also need excitations [25].

A constant speed wind turbine with a Doubly Fed Induction Generator (DFIG) is an asynchronous generator that uses two sets of windings the stator and the rotor to generate electrical output. The DFIG allows for better control of the electrical output, optimizing energy capture and ensuring stability. It operates over a wider range of wind speeds, ensuring optimal energy capture.

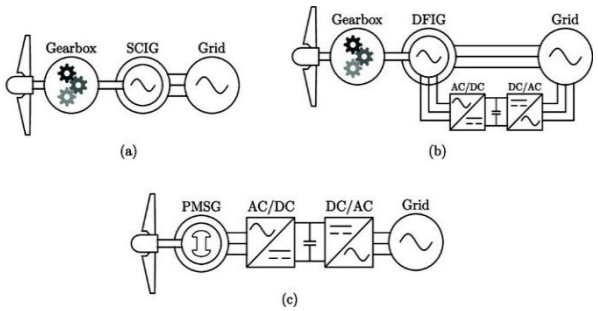


**Figure 7.** (a) A squirrel cage induction generator coupled with a constant speed wind turbine (SCIG), (b) a wind turbine with an incremental speed and a doubly fed induction generator (DFIG), and (c) A wind turbine with a permanent magnet synchronous generator and variable speed direct drive (PMSG) [28].

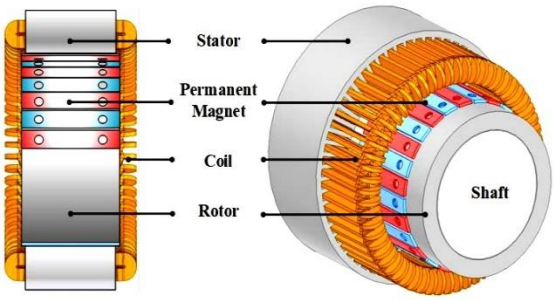


**Figure 8.** Analysis model of PMSG [29]

Additionally, it offers better fault ride-through capability, allowing it to stay on the grid even if there is a network disturbance as shown in Figure 7(b). Finally, the permanent magnet synchronous generator (PMSG) attracts researchers due to its better performance and reliability, better efficiency, and better fault ride-through (FRT) potential [26-27]. Reviews of WECS generators are given in [28-30]. As shown in Figure 7(c), Wind energy is converted into electricity using a permanent magnet synchronous generator (PMSG) and a variable speed direct drive wind turbine. This system uses a direct-drive configuration and a PMSG, reducing weight and complexity. The PMSG uses permanent magnets for a magnetic field, maximizing energy capture. Power electronics control generator speed and voltage output, as shown in Figure 8 these parts collectively form the PMSG, a synchronous generator known for its efficiency in wind energy conversion [31-32].

## 4. Modeling Wind Energy Conversion Systems (WECS).

Wind turbine generator (WTG) has climate change wind turbine, stable synchronous generator for power conversion with an uncontrolled three-phase rectifier. Learn about (AC/DC) power conversion.

### *4.1 Modeling of the wind turbine (WT)*

A wind turbine (WT) is a device that converts wind energy into mechanical energy. The output power of a wind turbine is given by [33]:

$$P_{turbine} = \frac{1}{2} C_p(\beta, \lambda) \rho \pi R^2 V_w^{\ 3} \quad (2)$$

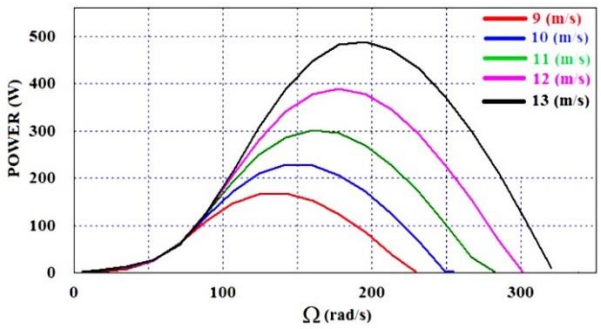


**Figure 9.** (WT) Relationship between output power and different level of wind speed [33]

where $\lambda$ is the tip speed ratio, β is the pitch angle, $C_p(\beta,\lambda)$ is the power coefficient, $V_w$ is the wind speed, $\rho$ is the air density, and $R$ is the radius of the (WT). $\beta$ is set to 0 in this work. The following defines the tip speed ratio:

$$\lambda = \frac{R\Omega_{turbine}}{V_w} \tag{3}$$

where $\Omega_{turbine}$ is the angular speed of the rotor (WT). The output power (WT) curves of wind turbines under different wind speeds are shown in Figure 9.

### *4.2 Permanent Magnet Synchronous Generator (PMSG) Modeling*

Because of their affordability and ease of use, these generator types are frequently utilized in small-scale generators (SWTG). The (PMSG) mathematical model is provided by [34].

$$v_q = -R_s i_q - L_q \frac{di_q}{dt} + \omega_e L_d i_d + \omega_e \lambda_m \tag{4}$$

$$v_d = -R_s i_d - L_d \frac{di_d}{dt} + \omega_e L_q i_q \tag{5}$$

where $R_s$ is the stator winding resistance; the direct axis and quadratic axis stator inductances are denoted by $L_d$ and $L_q$, respectively. $i_d$ and $i_q$ the current of the direct axis and quadratic axis respectively, The generator's amplitude and angular speed are represented by the variables $\omega_e$ and $\lambda_m$ flux connection, respectively. One way to define electromagnetic torque is as follows:

$$T_{em} = \left(\frac{3P}{2}\right)\left[\left(L_d - L_q\right) i_q i_d + i_q \lambda_m\right] \tag{6}$$

where $P$ represents the number of poles. The following expression (7) illustrates the link between mechanical angular speed $\Omega_{turbine}$ and electrical angular speed $\omega_e$ :

$$\omega_e = \frac{P}{2}\Omega_{turbine} \tag{7}$$

### *4.3 Modeling of three-phase uncontrolled rectifier*

A PMSG with a three-phase diode rectifier is depicted in Figure 10. The PMSG stator inductance is $L_s$ , and the stator resistance is $R_s$ . The phase a current voltage of the PMSG is determined by [35].

$$V_{an} = V_m \sin(\omega t) \tag{8}$$

where $V_m$ is the voltage level's maximum value. As demonstrated below, the generator's voltage and current determine the DC voltage and current output.

$$V_{dc} = \frac{3\sqrt{3}}{\pi} V_m \frac{3\sqrt{6}}{\pi} \lambda_{m-eff} P\Omega \tag{9}$$

$$I_{dc} = \frac{\pi}{\sqrt{6}} I_a \tag{10}$$

where $\lambda_{m-eff}$ is the flux linkages' amplitude (Wb). $I_a$ is the generator's output current (phase a), while $V_{dc}$ and $I_{dc}$ are the rectifier's average output voltage and current.

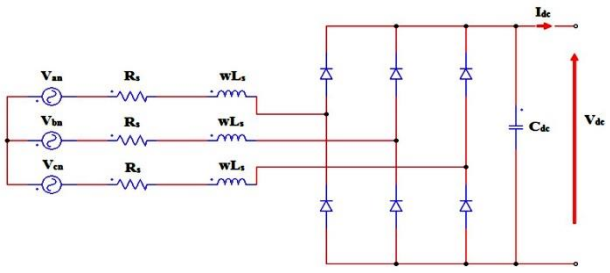


**Figure 10**. Three phase diode rectifier with PMSG

### *4.4 Modeling of three-phase interleaved buck-boost converter*

When the input current stops, inductors are employed to store energy because they recover quickly and the stored current is not phase-locked. Design of inductors and application of extra control ZVRT soft switching, inductor power outage, system volume, device switching loss, etc. It significantly affects the way the system performs. In order ensure that the inductor ripple current ($I_{Lp-p}$) is small, the inductor rating in a step-down converter is often selected to be large enough; In order to optimize output load current and decrease output ripple voltage, this is done [36]. The discontinuous mode can be connected to "light loads" in the case of high inductance values. Every design factor must be considered in order to maximize the inductor's performance. In general, the line between continuous mode (DCM) and continuous mode (CCM) can be used to determine the minimum inductance. Expressions from (11) to (15) can be used to explain the relationship between the inductor's peak current $I_{peak}$, minimum current $I_{\min}$, and root mean square (rms) current $I_{rms}$. The switching period $T_s$, load current (Id), load power $P$, and inductor current ripple $\Delta I$ are all included in this relationship [36].

$$\Delta I = \frac{1}{2}\frac{V_{in}-V_0}{L}\cdot\frac{V_0}{V_{in}}T_s \tag{11}$$

$$I_{load} = \frac{P}{V_o} \tag{12}$$

$$I_{peak} = I_{load} + \Delta I \tag{13}$$

$$I_{\min} = I_{load} - \Delta I \tag{14}$$

$$I_{rms} = \sqrt{I_{load}^2 + \frac{\Delta I^2}{3}} \tag{15}$$

It is forced to be zero for the inductance value. $I_{\min}$ is the value of this inductance allows the converter to operate in the CCM and DCM range.

$$L_{crit} = \frac{1}{2}\frac{(V_{in}-V_0)}{P}\cdot\frac{V_o^2}{V_{in}}T_s \tag{16}$$

$$L_{crit} = \frac{R(1-D)\cdot T_s}{2} \tag{17}$$

The inductor design must be optimized to meet the zero voltage switching condition and minimum switching frequency. Light loads will be affected by the non-continuous mode at large inductance values. Then the discontinuous conduction depends on the critical resistance $R_{crit}$.

$$R_{crit} = \frac{2L}{(1-D)T_s} \tag{18}$$

### *4.5 Proportional Integral Controller Modeling*

The system block diagram shown in Figure 11 is the basis for the controller developed for this technique. The current loops for the *d* and *q* axis are controlled by the same control loop. The conversion between $i_d$ and $v_d$ is given by [37].

$$\frac{I_{d,q}(s)}{V_{d,q}(s)} = \frac{1}{R_s}\frac{1}{1+T_e s} \tag{19}$$

Where the stator time constant is $T_e = \frac{L_{d,q}}{R_s}$

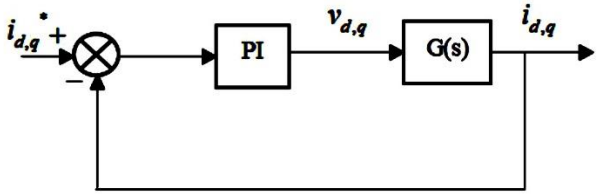


**Figure 11.** The proportional integral controller is defined as [37]

$$C(s) = \frac{k_i}{s}\left(1+\frac{k_p}{k_i}s\right) \tag{20}$$

The open loop compensation approach establishes the following PI controller parameters:

$$k_i = \frac{R_s^2}{L_{d,q}} \tag{21}$$

$$k_p = \frac{L_{d,q} k_i}{R_s} \tag{22}$$

The *d*,*q*-axis voltage reference $v_q^*$ and $v_d^*$ are created by adding the controller output and balancing time, resulting in a three-phase sinusoidal reference voltage. Thus, by separating the d and q voltages, the stator *d* and *q* currents are controlled. PWM is used to create a variable for power conversion. PI controllers are often used to control power output in maximum power point tracking (MPPT) wind turbines. However, PI controllers have robustness challenges in different environments. The challenges in Table 1 are summarized as follows:

**Table 1**: Robustness Challenges associated with PI controller [38-39].

| Robustness Issue | Explanation |
|---|---|
| Environmental Variations | Wind turbine systems operate in dynamic environments. Variations in wind direction and speed can have an impact on system performance and result in less than ideal power extraction. |
| Nonlinear Characteristics | Wind turbine dynamics exhibit nonlinearities. PI controllers may struggle to adapt to these nonlinear characteristics, resulting in less effective MPPT under certain conditions. |
| Modelling Inaccuracies | Inaccurate modeling of the wind turbine system can lead to discrepancies between the controller's expectations and the actual system response, impacting robustness. |
| Parameter Sensitivity | PI controllers are sensitive to parameter variations. Small changes in turbine or environmental parameters may lead to inadequate MPPT performance. |

### *4.6 Battery bank modeling*

Different battery modeling models were proposed in [33]. In this study, linear models were used as battery models. Models have ideal batteries with open voltage $E_o$ and balanced voltage, and an equivalent series resistance, $R_s$, The battery's terminal voltage is denoted by $V_{batt}$. By monitoring the open circuit and the charge of a completely charged battery, terminal voltage can be determined. The battery's linear structure is depicted in Figure 12. The formula for battery terminal voltage ( $V_{batt}$ ) can be expressed as this [33].

$$V_{battery} = E_o - I \cdot R_{Series} \tag{23}$$

where $E_o$ is the open circuit voltage of the battery and the current flowing through the battery., and $R_{Series}$ is the series resistance of the battery.

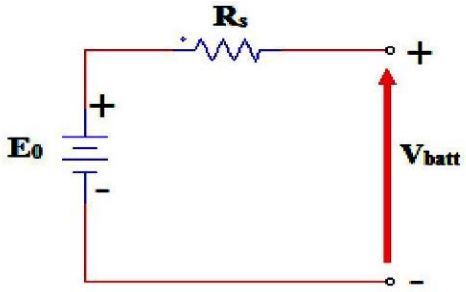


**Figure 12**. Basic schematic of the battery linear model

## 5. Implementing speed control with a three-phase interleaved buck-boost converter

The power output of a wind turbine can be determined by measuring the torque and rotational speed of the shaft. The system can be designed to vary the amount of air entering the turbine and see how the power output changes as wind speed increases or decreases. Optimum performance can be determined by collecting data on the relationship between shaft speed and power output at different speeds [40]. This information can be used to improve the turbine's efficiency and maximize electricity generation. To implement speed control, a three-phase interleaved buck-boost converter is developed.

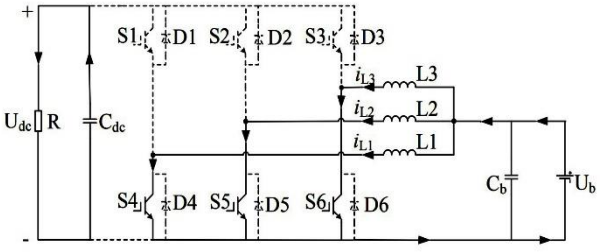


**Figure 13.** Equivalent circuit of three phase interleaved buck-boost converter [41]

This highly efficient DC-DC converter can handle high power levels and is suitable for power electronics applications like wind turbine power output tracking systems. By controlling the duty cycle, the converter can adjust the output voltage or current and regulate the power output to match the desired output power. The equivalent interleaved circuit as shown in Figure 13, reduces current and voltage stress on each switch, resulting in lower switching losses and higher efficiency. Using a three-phase interleaved buck-boost converter in a wind turbine power output tracking system can improve efficiency, reliability, and precise control of the turbine's output power [41]. The following can be used to represent the relationship between the input and output voltages:

$$U_{dc} = \frac{1}{1-D} U_b \tag{24}$$

## 6. MPPT technique for wind energy conversion system

### *3.1 Perturbation and Observation Algorithm for Wind Turbine*

In addition, the circuit is to have a three-phase diode bridge, used at the input. This ensures that only one diode phase is on at a time, making it so that the most positive voltage is input at any given time. A permanent magnet synchronous generator is to be inputted into the three-phase rectifier. Once the circuit has been developed, the proper gain value for the circuit that allows for the generator speed to be tracked is to be found. This is done by trying different values for gain until a plot is seen where the measured speed stabilizes to the reference speed. Negative gain is to be used because there is an inverse relationship between speed and current. For example, if the reference speed is higher than the measured speed, the power pulled will be decreased as well as the current so that the speed can be increased. After this gain value has been found, the system must be used to verify the speed control for multiple input speeds. Maximum PowerPoint Tracking is implemented using Perturbation and Observation [42]. To implement MPPT, the schematic needs the following updates: change from constant reference speed input to simplified C-block on PSIM with the inputs speed and power and change from constant torque input to wind turbine input with a speed of 12m/s.

A Simplified C-block is used to program the logic for MPPT. Two two-layer nested conditional statements will be used to emulate a MUX-like system when it comes to changes in reference speed. Taking current power output and current speed as input, the MPPT will compare those against the previous power output and previous speed. With these comparisons, the system can deduce change in power (denoted as $P(n)-P(n-1)$) and change in speed (denoted as $\omega(n)-\omega(n-1)$) in Figure 3.

The MPPT is then to be tested with multiple delta values that change how much the speed is being perturbed each iteration [43]. The MPPT method is represented by the flow chart diagram in Figure 3. Different perturbation delta values are to be tested for the speed (corresponding to "Decrease $\omega_{ref}$" or "Increase $\omega_{ref}$" in the flow chart diagram)

## 7. Methodology

### *7.1 Speed control implementation*

Once the shaft speeds were found for the wind turbine, the next step is to implement speed control into the three-phase Buck-Boost converter as described above. The schematic in Figure 14 is developed and used for the simulations for speed control implementation, with only the gain on the speed control PI being adjusted [44].

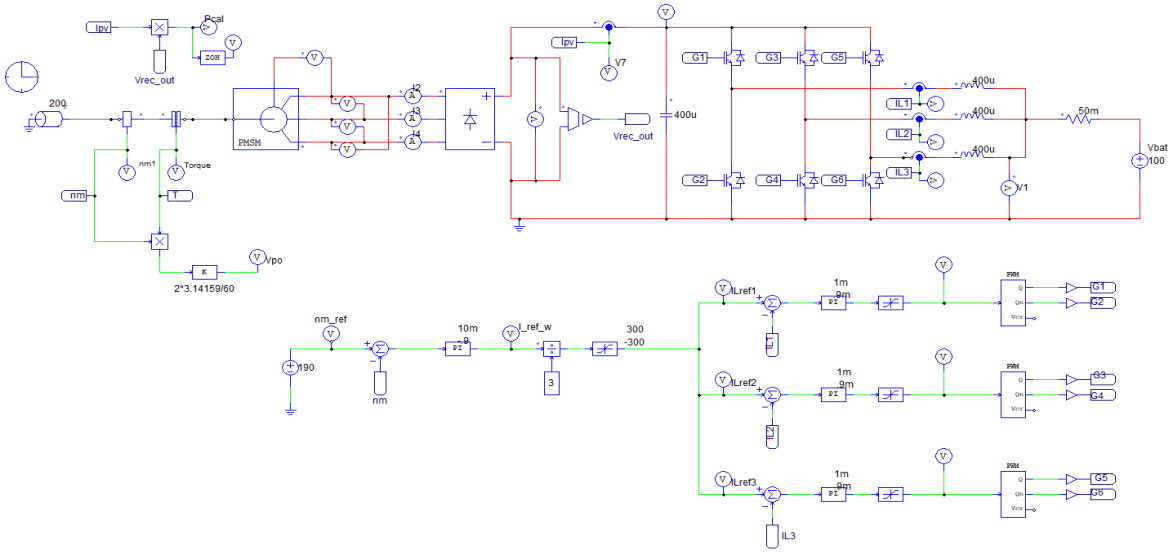


**Figure 14.** Schematic for speed control implementation

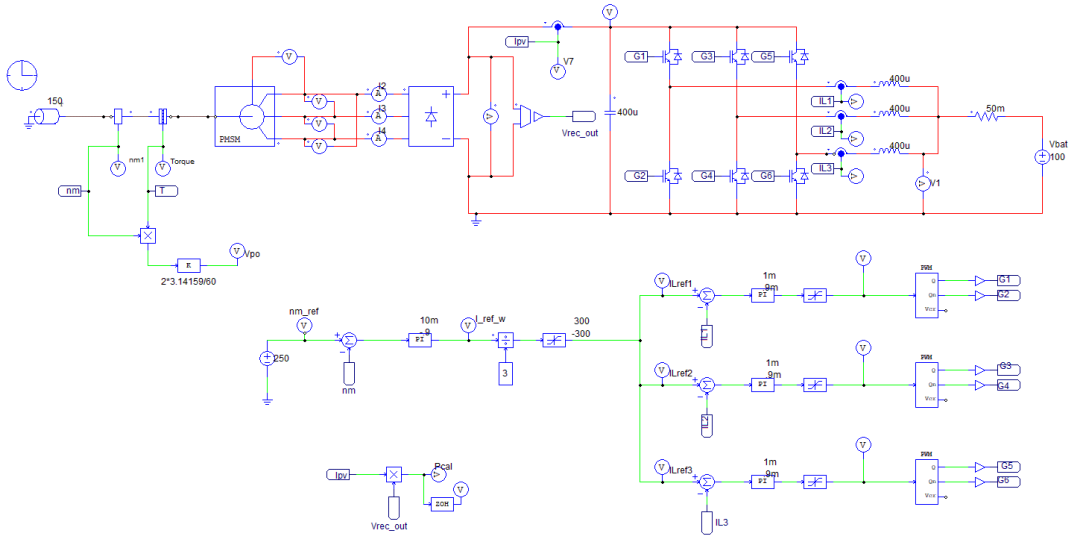


**Figure 15.** Schematic for speed control implementation with changed reference speed and torque

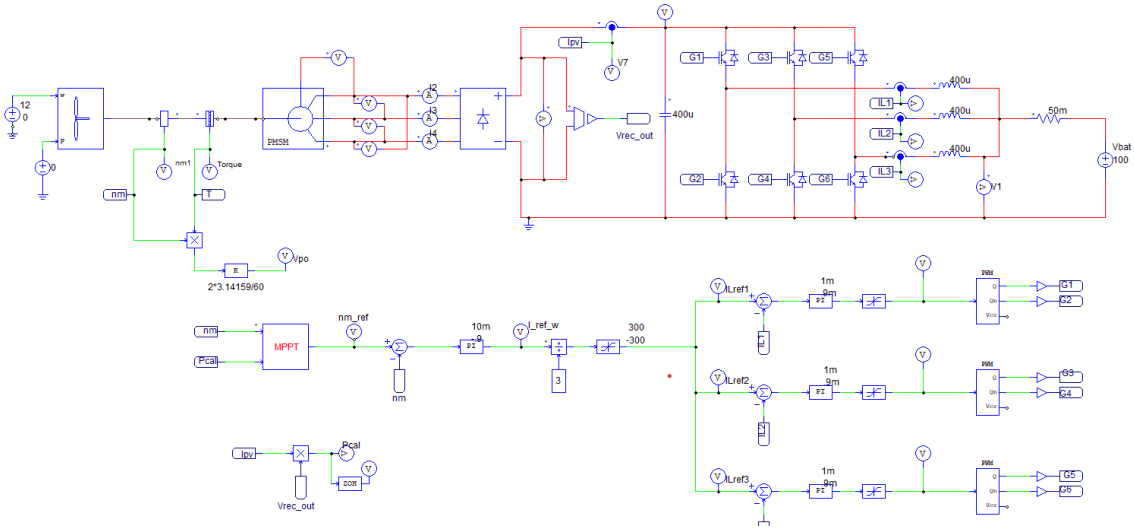


**Figure 16.** Schematic for MPPT implementation

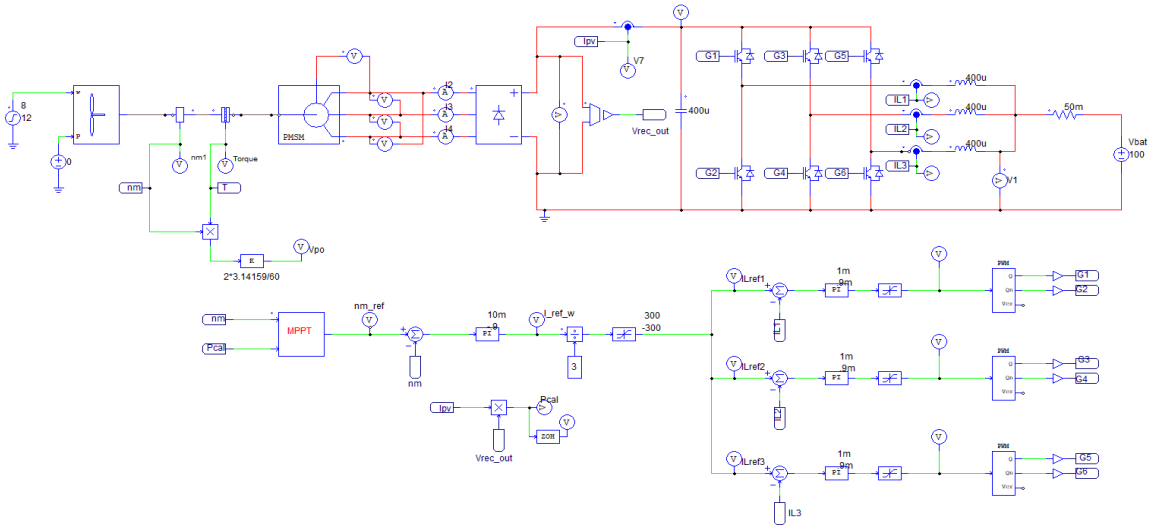


**Figure 17.** Schematic for MPPT verification with changing input speed from 12m/s to 8m/s

### *7.2 Speed control implementation with changed reference speed and torque*

To verify these results, the speed control was tested for a new torque of 150 and a reference speed of 250 rad/sec. The schematic is shown in Figure 15.

### *7.3 MPPT implementation*

Once the speed control is implemented, the next step is implementing maximum power point tracking. The constant input is changed to a simplified C-block and the constant torque input is changed to a wind turbine. For this step, a wind speed of 12*m/s* is used for the wind turbine as shown in Figure 16. Once the code was implemented in the C block as described above, the delta values that adjust how much the system is perturbed, need to be adjusted [45].

### *7.4 MPPT verification with changing input speed from 12m/s to 8m/s*

The next step is to test the MPPT when changing the wind speed from 12*m/s* to 8*m/s*. First, the MPPT that is use in the previous step is test with the new step input. The PSIM schematic is changed to have a step input that changes the speed from 12*m/s* to 8*m/s* rather than the constant speed input [46]. The schematic for this update circuit is shown in Figure 17.

## 8. Simulation results and discussion

The first gain used is -0.4 which produced the plot in Figure 18. The speed stabilizes, but a system that stabilizes quicker than ~0.6 seconds, as seen here, would be ideal. The reference speed is 190 rad/sec and the input torque is 200 Nm. The gain is changed from -0.4 to -0.9 to increase the stabilization time. As seen in Figure 18 and Figure 19, the overshoot increased, but the second and subsequent peaks were reduced by about 25W and the total stabilization time was about 0.4s less. As seen in Figure 20, the speed does stabilize, but not as quickly as for the previous input. There are some MPPT approaches compared and analyzed is shows in Table 3.

The plot in Figure 21 illustrates the result from using a delta value of 0.005. The power does not stabilize at the expected value of 19kW at all within 0.1s, so a new delta value was tried. It is also seen that the reference speed diverges, meaning the issue is likely with our code, rather than with our gain [47]. The negative delta value (corresponding to decreasing speed) is changed from 0.005 to -0.0005 and the positive delta value (corresponding to increasing speed) is kept at 0.005. The results from this simulation are displayed in Figure 22, which is initially run at 0.1s, so the running time would not take too long, but an improvement is already visible in that the power does not decrease to 0W. The plot in Figure 23 shows the same simulation run for

0.2s showing that these delta values do allow the system to stabilize at the goal power of 19kW. Aiming for a quicker stabilization time, more simulations were run. Figure 24 shows the results for the next delta values used (Negative Delta: -0.00005, Positive Delta: 0.005).

The negative delta was decreased to remove the steep drop at around 50ms. As seen in the result, this did not work and the system did not stabilize at all in the given time and diverged from the intended value of 19kW. The reference speed is incorrect here as well and consistently increasing. Following this, the decision was to have the negative delta (absolute value) decrease from 0.0005 and increase from 0.00005 to find a midway point. Using these new values (Negative Delta: -0.0002, Positive Delta: 0.005) the results shown in Figure 25 are found, where it is seen that the power stabilizes at 19kW and takes about 0.3s.

This is an increase from the stabilization time in a previous result, so the previous result was retested to verify that it was the most efficient. The results in Figure 26 show the retested results (Negative Delta: -0.0005, Positive Delta: 0.005) with the system stabilizing correctly at 19kW in about 0.15s. This resulted in the decision to keep these delta values for this stage and begin the next stage of changing the speed from 12m/s to 8m/s. This resulted in the plot in Figure 27 where the power oscillates greatly around the goal speed of 5.6kW. This is not ideal because the aim is to have a system with fewer oscillations at the goal power.

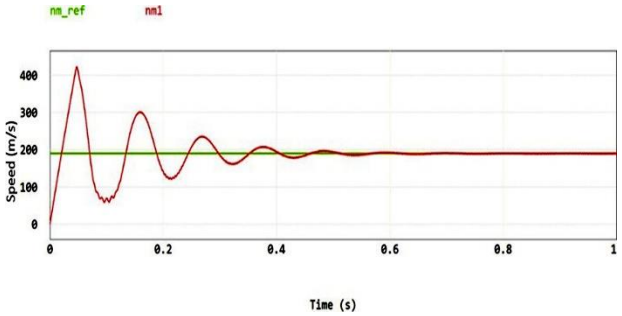


**Figure 18.** Speed control results for Gain = -0.4

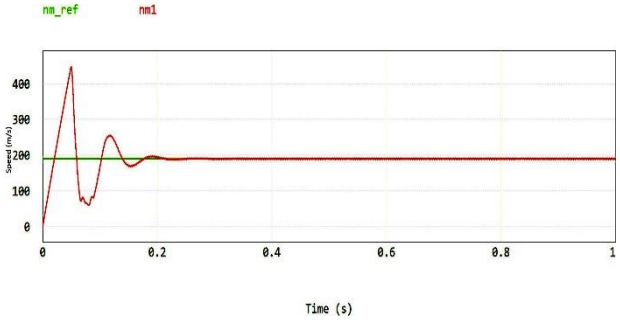


**Figure 19.** Speed control results for Gain = -0.9

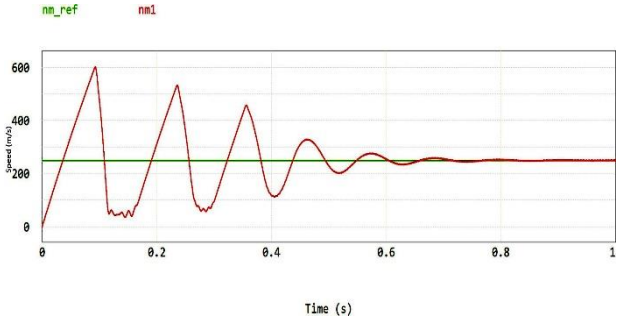


**Figure 20.** Speed control results for Gain = -0.9 for New Input Speed and Torque

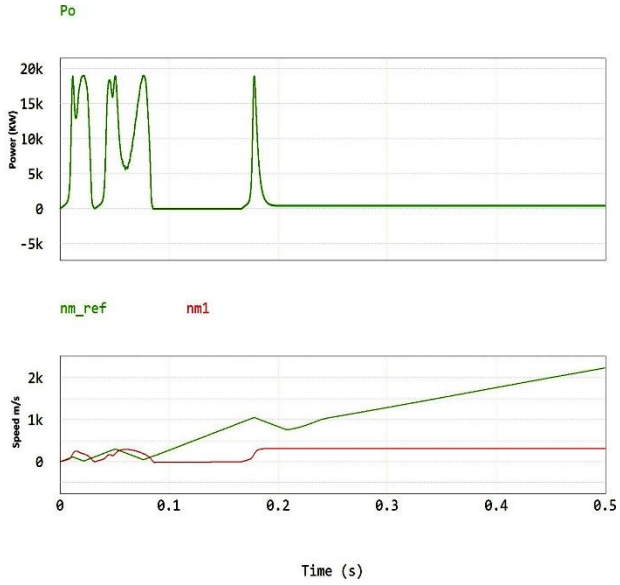


**Figure 21.** Output power results for delta = 0.005

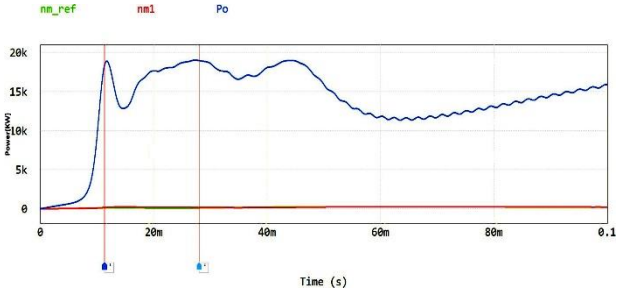


**Figure 22.** Output power results for negative delta: -0.0005, Positive Delta: 0.005

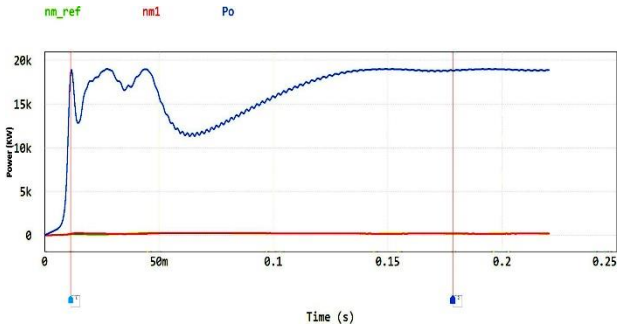


**Figure 23.** Output power results for negative delta: -0.0005, positive delta: 0.005 (same as above, but run for more time to show longer term results)

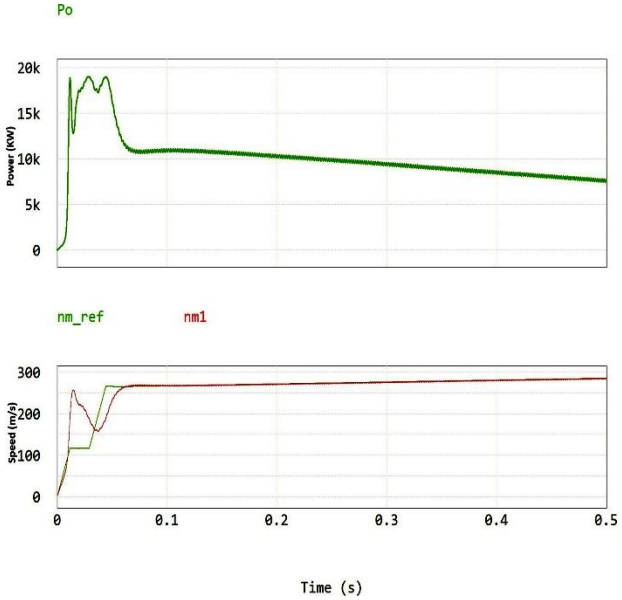


**Figure 24.** Output power and speed results for negative delta: -0.00005, positive delta: 0.005

The speed is still being track relatively well, although the speed changed many times as shown in Figure 28. The delta values were adjusted to attempt to get rid of the oscillations in power. The negative delta value was changed to -0.0002, so the decrease would not be as drastic, and the result is displayed in Figure 29. The speed shows one step and then settles at around 130 rad/sec as expected from earlier simulations for turbine characteristics in Figure 30.

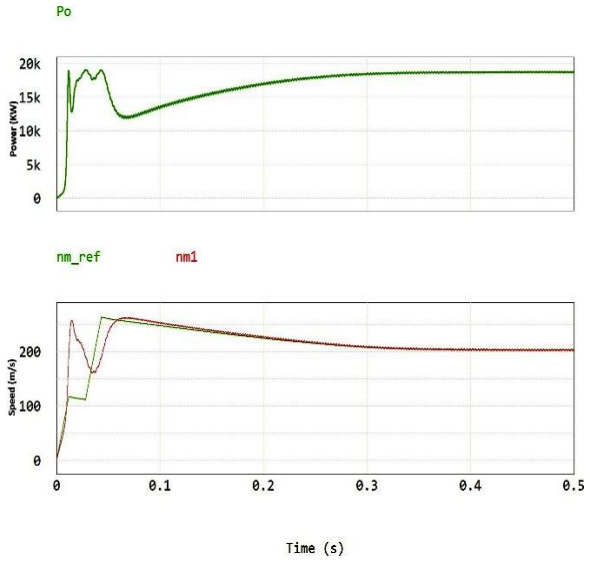


**Figure 25.** Output power and speed results for negative delta: -0.0002, positive delta: 0.005

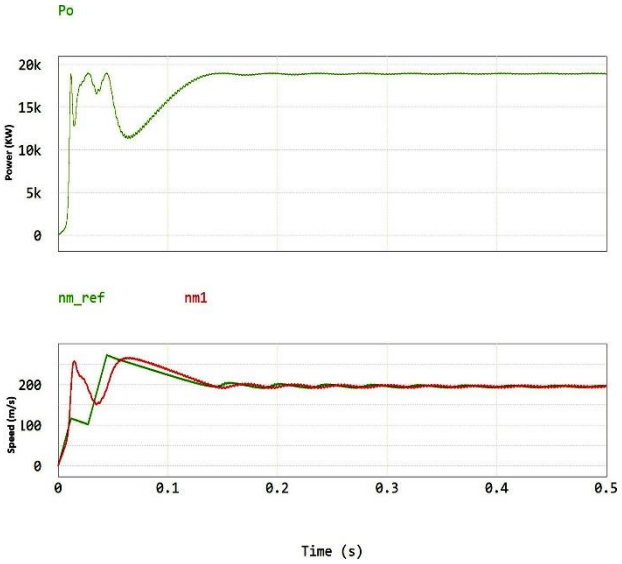


**Figure 26.** Output power and speed results for negative delta: -0.0005, positive delta: 0.005

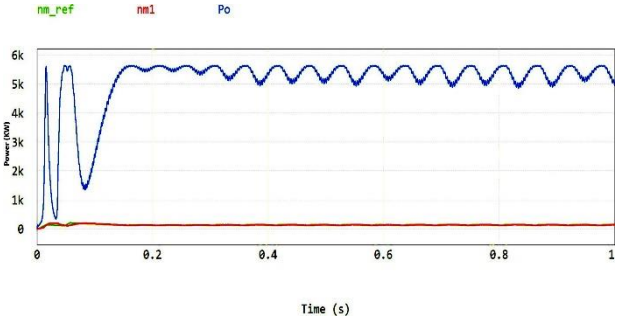


**Figure 27.** Power output with negative delta: -0.0005, positive delta: 0.005

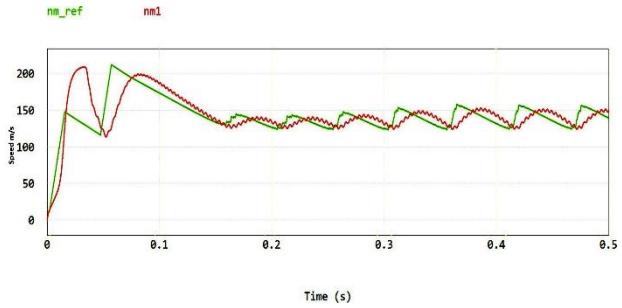


**Figure 28.** Measured speed and reference speed with negative delta: -0.0005, positive delta: 0.005

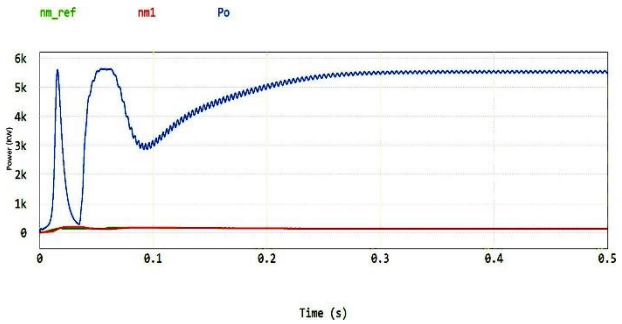


**Figure 29.** Power and speed output with negative delta: -0.0002, positive delta: 0.005

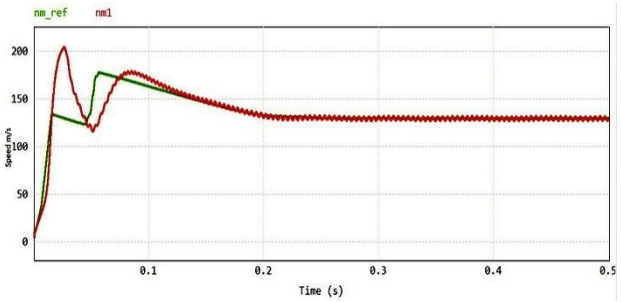


**Figure 30.** Measured speed and reference speed with negative delta: -0.0002, positive delta: 0.005

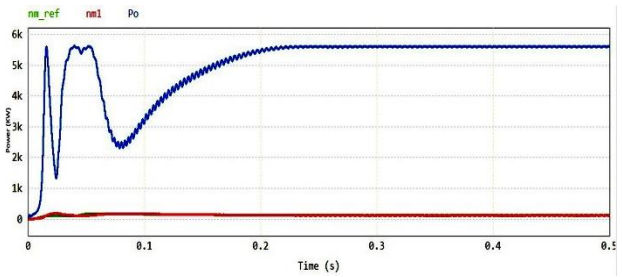


**Figure 31.** Measured speed and reference speed with negative delta: -0.0002, positive delta: 0.005 (with Near-Zero Implementation)

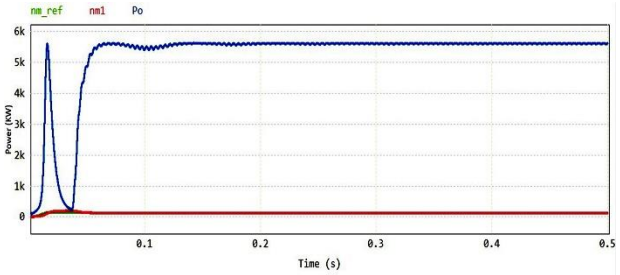


**Figure 32.** Power output with negative delta: -0.0002, positive elta: 0.0065 (with Near-Zero Implementation)

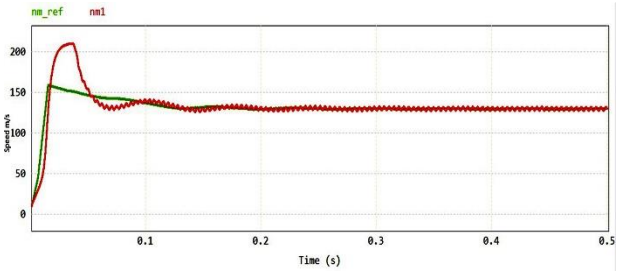


**Figure 33.** Measured speed and reference speed with negative delta: -0.0002, positive delta: 0.0065 (with Near-Zero Implementation)

## 9. Near zero implementation in Maximum Power Point Tracking (MPPT)

New-zero implementation technique is a type of maximum power measurement (MPPT) algorithm for wind turbines. It is based on the idea that the ideal tip speed ratio (TSR) of a wind turbine is nearly constant and can be estimated by measuring the wind speed and turbine speed. This algorithm adjusts the duty cycle of the three-phase interleaved buck-boost converter to control the turbine speed and match the TSR effectively. This technique can improve the power extraction and efficiency of the wind turbine under different wind conditions. In the simplified C-block logic for MPPT, a smart feature is added. In the previous logic, if a change in power is equal to 0, no delta changes would be made. Now with the new smart logic, if the change in power is a value small enough, the MPPT will consider that to be 0 (Appendix 31 CODE, Line 29). This is done to minimize pulsing at the peak power level. The "small enough" value chosen was 0.02 (Appendix CODE, Line 24). For the MPPT system to make positive and negative delta changes, the absolute value of the change in power must be greater than 0.02.

It is also observed that the power output approaches peak power faster than before. Continuing to optimize the MPPT system, additional delta changes were made. The goal is to remove the second power spike and allow the system to reach peak power and become stable in less time, with this extra feature, it is observed that power at the peak is smoother with smaller ripples as shown in Figure 32 than the larger ripples observed before as shown in Figure 29. It also measured speed and reference speed with Near-Zero Implementation and successfully met the reference speed as shown in Figure 33.

## 10. Comparisons analysis

*10.1 Implementing the smart system (Near-Zero Implementation)* [48-49]

*10.1.1 Faster peak power approach*

a) Previously, it took approximately 0.3 seconds to reach peak power as shown in Figure 29.
b) Now, it takes approximately only 0.06 seconds to reach peak power as shown in Figure 31.

*10.1.2 Less power spikes*

a) Previously, two large power spikes were observed as shown in Figure 29.
b) Now, one large power spike is observed as shown in Figure 31.

*10.1.3 Less peak power rippling*

a) Previously, peak power had larger and more jagged/sharp ripples as shown in Figure 29.
b) Now, peak power has smaller and smoother ripples as shown in Figure 31.

The optimization aims to smoothen the power ramp-up enough to be considered "removed." The comparison of before and after near zero implementation with same delta values optimized delta values are shows in Table 2 and Table 4.

**Table 2:** Before and after near zero implementation with same delta values

| Delta approach | Before Near Zero Implementation | With Near Zero Implementation |
|---|---|---|
| Positive Delta Value | 0.005 | 0.005 |
| Negative Delta Value | -0.0002 | -0.0002 |
| Peak Power Approach | 0.3 | 0.22 |
| Peak Power Rippling | Larger and more jagged ripples | Smaller and smoother ripples |

**Table 3:** Dynamic performance of evaluated MPPT approaches compared and analyzed. [50]

| MPPT techniques | Complexity | Sensed parameters | Converges speed | Settling time (sec) | Efficiency (%) |
|---|---|---|---|---|---|
| P&O with Interleaved Buck-Boost Converter | Moderate | Voltage and current | Fast | 0.356 | 96.8 |
| P & O with Buck converter | Low | Voltage | Moderate | 0.365 | 95.3 |
| P & O with Sync Buck converter | Low | Voltage | Moderate | 0.376 | 96.5 |
| INC with Buck converter | Moderate | Voltage and current | Fast | 0.361 | 95.4 |

**Table 4**: Before and after near zero implementation with optimized delta values

| Delta approach | Before Near Zero Implementation | With Near Zero Implementation |
|---|---|---|
| Positive Delta Value | 0.005 | 0.0065 |
| Negative Delta Value | -0.0002 | -0.0002 |
| Peak Power Approach | 0.3 | 0.06 |
| Number of Power Spikes | 2 | 1 |
| Peak Power Rippling | Larger and more jagged ripples | Smaller and smoother ripples |

## 11. Conclusions

A wind turbine has been successfully implemented with speed control and maximum power point tracking (MPPT) using a three-phase interleaved buck-boost converter and a permanent magnet synchronous generator. The system is tested at various input speeds and perturbation delta values to optimize performance. Results showed that a gain value of -0.9 reduced the stabilization time to 0.4 seconds and reduced subsequent peaks by 25W. The system can be optimized to reduce stabilization time while maintaining stable output. For MPPT implementation, an initial delta value of 0.005 did not allow the system to stabilize at the expected power of 19 kW within 0.1 seconds. However, by changing the negative delta value to -0.0005, the system was able to stabilize at the goal power of 19 kW within 0.2 seconds. By combining these approaches, we have achieved a synergistic effect, leading to improved stability and performance of wind turbines. These findings hold promising implications for the renewable energy sector, offering a pathway to harnessing wind power more reliably and efficiently. By implementing the proposed techniques, wind energy can become a more reliable and viable source of renewable energy, further contributing to the global efforts towards a sustainable and low-carbon future.

## References

[1] New installed wind energy capacity worldwide 2022 |Statista." *New installed wind energy capacity worldwide 2022 | Statista*. October 2023.

[2] Global installed wind energy capacity 2022 | Statista. (2023c,). *Global cumulative wind energy installed capacity*. August 29

[3] Alex. (2023b, October 9). Global Offshore Wind Report. *Global Wind Energy Council*. https://gwec.net/gwecs-global-offshore-wind-report-2023

[4] Lawan, Muhammad, Ahmed Aboushady, and Khaled H. Ahmed. "Photovoltaic MPPT Techniques Comparative Review." *2020 9th International Conference on Renewable Energy Research and Application (ICRERA)*. 2020. 344-351

[5] Y. Vidal, L. Acho, N. Luo, M. Zapateiro and F. Pozo, "Power Control Design for Variable-Speed Wind Turbines," *Energies*, vol. 5, p. 3033–3050, 2012.

[6] Badawi, A. Samir "Paper review: maximum power point tracking for wind energy conversion system." *2020 2nd International Conference on Electrical, Control and Instrumentation Engineering (ICECIE)*. 2020. 1-6.

[7] Mousa, Hossam H. H.,. "State of the art perturb and observe MPPT algorithms based wind energy conversion systems: A technology review." *International Journal of Electrical Power & Energy Systems* 126 (March 2021): 1-8

[8] Abdullah, Mokhtar, A. H. M.. "A review of maximum power point tracking algorithms for wind energy systems." *Renewable & Sustainable Energy Reviews* 16 (June 2012): 3220–3227

[9] A. Musyafa, I. Abadi, R. Noriyati, "Design and Implementation Wind Turbine Power Control System Base Particle Swam Optimization at Low Rate Wind Farm," *International Journal of Mechanical & Mechatronics Engineering*, vol. 19, p. 149–157, October 2019

[10] Xu, Changzhi, et al. "Time-frequency analysis-based deep interference classification for frequency hopping system." *EURASIP Journal on Advances in Signal Processing* September 2022.

[11] Gangavarapu, Sivanagaraju, and Akshay Kumar Rathore. "Analysis and Design of Three-Phase Interleaved Buck-Boost Derived PFC Converter."

2019 *IEEE Industry Applications Society Annual Meeting*. 2019. 1-8.

[12] O. Apata and D. T. O. Oyedokun, "An overview of control techniques for wind turbine systems," *Scientific African,* vol. 10, p. e00566, 2020.

[13] Kaouane, Mohamed, A. Boukhelifa. "Regulated output voltage double switch Buck-Boost converter for photovoltaic energy application." *International Journal of Hydrogen Energy* 41 (December 2016): 20847–20857.

[14] Huangfu, Yigeng, Ronghua Ma, Bo Liang, and Yuren Li. "High power efficiency BucK Converter design for standalone wind generation system." *International Journal of Antennas and Propagation* 2015 (January 2015): 1–9.

[15] H.Taufik, M.Efendi,. "Maximum Power Point Tracking Interleaved Boost Converter Using Cuckoo Search Algorithm on The Nano Grid System." *JAREE (Journal on Advanced Research in Electrical Engineering)* 5 (April 2021)

[16] Raghavendra, Kummara Venkata Guru, et al. "A Comprehensive Review of DC–DC Converter Topologies and Modulation Strategies with Recent Advances in Solar Photovoltaic Systems." *Electronics* 9 (December 2019): 31

[17] Pande, Ketan Kotecha, and Vijayakumar Varadarajan. "A review of maximum power point tracking Algorithms for wind energy conversion systems." *Journal of Marine Science and Engineering* 9 (October 2021): 1187.

[18] Elkodama, Amira, Amr Ismaiel, A. Abdellatif, S. Shaaban, Shigeo Yoshida, and Mostafa A. Rushdi. "Control Methods for Horizontal Axis Wind Turbines (HAWT): State-of-the-Art Review." *Energies* 16 (September 2023): 6394.

[18] Mousa, Hossam H. H. "State of the art perturb and observe MPPT algorithms based wind energy conversion systems: A technology review." *International Journal of Electrical Power & Energy Systems* 126 (March 2021): 106598.

[19] Baba, Ali Omar, Guangyu Li, and Xiaohui Chen. "Classification and Evaluation Review of maximum power point tracking methods." *Sustainable Futures* 2 (January 2020): 100020.

[20] Zhang, Xinyue, and Ershuai Li. "A Novel Method Based on Time-Frequency Modeling for Interference Analysis in Avionics Systems." 2022 *IEEE 41st Digital Avionics Systems Conference (DASC*). 2022. 1-8.

[21] Kumar, Dipesh, and Kalyan Chatterjee. "A review of conventional and advanced MPPT algorithms for wind energy systems." *Renewable & Sustainable Energy Reviews* 2020: 957–970.

[22] A. Musyafa, I. Abadi, R. Noriyati, M. Faiz and M. Asy'ari, "Design and Implementation Wind Turbine Power Control System Base Particle Swam Optimization at Low Rate Wind Farm," *International Journal of Mechanical & Mechatronics Engineering,* vol. 19, p. 149–157, October 2019

[23] S. Roga, S. Das, S. Datta, V. Kisku and S. Bardhan, "Energy Converters for Wind Turbines: Implementation of Control Methods," in *2022 IEEE International Conference on Power Electronics, Drives and Energy Systems (PEDES)*, 2022

[24] Beainy, N. Moubayed, and Fouad Kaddah. "Comparison of different types of generator for wind energy conversion system topologies." 2016 3rd *International Conference on Renewable Energies for Developing Countries (REDEC).* 2016. 1-6.

[25] Gamal, Haytham, and A. Shaltout. *Maximum output power of wind energy system combined with battery energy storage using rule-based control*. 2021.

[26] Muller, S., M. Deicke, and R. W. De Doncker. "Doubly fed induction generator systems for wind turbines." *IEEE Industry Applications Magazine* 8 (2002): 26-33.

[27] Molina, Marcelo, and Pedro Mercado. "Modelling and Control Design of Pitch-Controlled Variable Speed Wind Turbines." 2011.

[28] De Kooning, Jeroen D. M., , and Lieven Vandevelde. "Digital Twins for Wind Energy Conversion Systems: A literature review of potential modelling techniques focused on model fidelity and computational load." *Processes* 9 (December 2021): 2224

[29] Hong, Ji-Su, Hoon-Ki Lee, Junghyo Nah, Kyong- "Semi-3D analysis of a permanent magnet synchronous generator considering bolting and overhang structure." *Energies* 15 (June 2022): 4374.

[30] Bhutto, Darya Khan, and Faheem Akhtar Chachar. "WIND ENERGY CONVERSION SYSTEMS (WECS) GENERATORS: A REVIEW." 2019 2nd *International Conference on Computing, Mathematics and Engineering Technologies (iCoMET)*. 2019. 1-6.

[31] Alkul, Oguz, Dabeeruddin Syed, and Sevki Demirbas. "A Review of Wind Energy Conversion Systems." 2022 10th *International Conference on Smart Grid (icSmartGrid).* 2022. 72-77.

[32] Ulutaş, Alper, and Tarik Duru. "Variable-Speed Direct-Drive Permanent Magnet Synchronous Generator wind turbine modeling and simulation." Kocaeli journal of science and engineering 2 (May 2019): 21–27.

[33] Jaballah, Mohamed Akram, and Abdelkader Mami. "Design and Simulation of Robust Controllers for Power Electronic Converters used in New Energy Architecture for a (PVG)/ (WTG) Hybrid System." *International Journal of Advanced Computer Science and Applications* 8 (January 2017).

[34] Louar Fateh, Djellad Abdelhak And Bouras Lakhdar, “Modeling and control of a permanent magnet synchronous generator dedicated to standalone wind energy conversion system”,*Frontiers in Energy*, Vol.10, No.2, , June 2016. 155-163

[35] D. W. Hart, “Power Electronics’, McGraw Hill, 2011

[36] Nandankar, Praful, and Jyoti Rothe. "Design and implementation of efficient three-phase interleaved DC-DC converter." 2016. 1632-1637.

[37] A. Hammami, I. Saidi and D. Soudani, "Comparative Study of PMSG Controllers for Variable Wind Turbine Power Optimization," *International Journal of Advanced Computer Science and Applications*, vol. 9, January 2018.

[38] A. Mseddi, S. L. Ballois, H. Aloui and L. Vido, "Robust control of a HESG for a wind energy application," *Electric Power Systems Research*, vol. 168, p. 250–260, March 2019.

[39] P. Chen, D. Han and K. Li, "Robust adaptive control of maximum power point tracking for wind power system," *IEEE Access*, vol. 8, p. 214538–214550, January 2020.

[40] E. C. Navarrete, M. T. Perea, J. C. J. Correa, R. V. C. Serrano and G. J. R. Moreno, "Expert Control Systems Implemented in a Pitch Control of Wind Turbine: A Review," *IEEE Access*, vol. 7, 2019, p. 13241–13259

[41] B. Xie, Y. Ji, J. Wang, H. Wang, and C. Ma, ‘Modeling and control for a three-phase interleaved bidirectional DC-DC energy storage converter’, in 2017 China *International Electrical and Energy Conference (CIEEC)*, 2017, pp. 153–158.

[42] S. Musumeci, R. Bojoi, E. Armando, S. Borlo and F. Mandrile, "Three-Phases Interleaved Boost Power Factor Corrector for High-Power LED Lighting Application," *Energies*, vol. 13, 2020.

[43] X. Li, J. Qian, D. Tian, Y. Zeng, F. Cao, L. Li and G. Zhang, "Maximum Power Tracking Control of Wind Turbines Based on a New Prescribed Performance Function," *Energies*, vol. 16, 2023.

[44] M. Bereš, D. Kováč, T. Vince, I. Kováčová, J. Molnár, I. Tomčíková, J. Dziak, P. Jacko, B. Fecko and Š. Gans, "Efficiency Enhancement of Non-Isolated DC-DC Interleaved Buck Converter for Renewable Energy Sources," *Energies*, vol. 14, 2021.

[45] J. Pande and P. Nasikkar, "A Maximum Power Point Tracking Technique for a Wind Power System Based on the Trapezoidal Rule," *Energies*, vol. 16, 2023.

[46] S. Rajput, M. Averbukh, A. Yahalom and T. Minav, "An Approval of MPPT Based on PV Cell’s Simplified Equivalent Circuit During Fast-Shading Conditions," *Electronics*, vol. 8, 2019.

[47] S. Jiao, D. Patterson and S. Camilleri, "Boost converter design for 20kW wind turbine generator," *International Journal of Renewable Energy Engineering*, vol. 2, January 2000.

[48] S. Karyś and P. Stawczyk, "Cost-Effective Power Converters for Small Wind Turbines," *Energies*, vol. 14, 2021..

[49] Y. Yang and S. C. Tan, "Trends and Development of Sliding Mode Control Applications for Renewable Energy Systems," *Energies*, vol. 12, 2019.

[50] M. Lawan, A. Aboushady, and K. H. Ahmed, ‘Photovoltaic MPPT Techniques Comparative Review’, in 2020 9th *International Conference on Renewable Energy Research and Application (ICRERA)*, 2020, pp. 344–351.

## Table of acronyms

| Abbreviations | Full Form |
|---|---|
| MPPT | Maximum Power Point Tracking |
| GWEC | Global Wind Energy Council |
| AC | Alternating Current |
| DC | Direct Current |
| PI | Proportional-Integral |
| WECS | Wind Energy Conversion Systems |
| SCIG | Squirrel cage asynchronous generators |
| DFIG | Doubly fed asynchronous generators |
| PMSG | Permanent Magnet Synchronous Generator |
| FRT | Fault ride-through |
| WTG | Wind turbine generator |
| SWTG | Small wind turbine generator |
| ZVRT | Zero-voltage ride through |
| DCM | Discontinuous conduction mode |
| CCM | Continuous conduction mode |
| PWM | Pulse Width Modulation |
| RMS | Root-mean-square |
| TSR | Tip speed ratio |
| P & O | Perturb and Observe |
| INC | Incremental conductance |
| EMF | Electromotive force |

## MPPT PSIM Code for Simplified C-Block

```
//MPPT algorithim
//Initialize values
static double nm;
static double nm_old;
static double nm_ref;
static double nm_delta;
static double Pcal;
static double Pcal_old;
static double Pdelta;
// Probe
nm = x1; // Input 0 = Vov
Pcal = x2; // input 1 = Ipv

//Ppv = Vpv * Ipv; // Calculate New power output
Pdelta = Pcal - Pcal_old; // Power Delta

// New Voltage Probed - Old Voltage Probed
nm_delta = nm - nm_old;

//MPPT Algorithm with Near-Zero implimentation
//if Pdelta is between range/threshold small enough to consider it 0 (to lessen zig zag at peak level)
// if Pdelta is between 'nearzero' and negative 'nearzero', then consider that closer enough to be 0

double nearzero = 0.02; // initialize neazero.
// A larger 'nearzero' means more range/threshold around 0 is considered to be 0.
// A smaller 'nearzero' means less range/threshold around 0 is considered to be 0.

// Cond 1: Change in power is 0 or extremely close to 0. No changes made.
if (Pdelta<nearzero && Pdelta >-1*nearzero){
    return;}

// Cond 2: Change in power is positive beyond near-zoro range/threshold. Changed will be made.
else if (Pdelta > 0){
    if(nm_delta > 0){ // Condition 2.1: Change in speed is positive
        nm_ref = nm_ref + 0.0065;}
    else // Condition 2.2: Change in speed is 0 or negative
        nm_ref = nm_ref - 0.0002;}

// Cond 3: Change in power is negative beyond near-zoro range/threshold. Changed will be made.
else if (Pdelta < 0){
    if(nm_delta < 0){ // Condition 3.1: Change in speed is negative
        nm_ref = nm_ref + 0.0065;}
    else // Condition 3.2: Change in speed is 0 or positive
        nm_ref = nm_ref - 0.0002;}

Pcal_old = Pcal; // Save current power for next step
nm_old = nm; // Save current speed for next step

y1=nm_ref; // Output
```